Temperature-Dependent Electrical and Ultrastructural Characterizations of Porcine Skin upon Electroporation

Stephen A. Gallo, Arindam Sen, Mary L. Hensen, and Sek Wen Hui
Membrane Biophysics Laboratory, Department of Molecular and Cellular Biophysics, Roswell Park Cancer Institute, Buffalo, New York 14263 USA

ABSTRACT The mechanism of high-voltage pulse-induced permeabilization of the stratum corneum, the outer layer of the skin, is still not completely understood. It has been suggested that joule heating resulting from the applied pulse may play a major role in disrupting the stratum corneum. In this study, electrical and ultrastructural measurements were conducted to examine the temperature dependence of the pulse-induced permeabilization of the stratum corneum. The stratum corneum resistance was measured using a vertical diffusion holder, with the stratum corneum placed between two electrode-containing chambers. The stratum corneum resistance was reduced manyfold during the applied pulse. The extent of resistance reduction increased with pulse voltage until reaching a threshold value, above which the resistance reduction was less dependent on the pulse voltage. The stratum corneum was more susceptible to permeabilization at high temperature, the threshold voltage being lower. The stratum corneum resistance recovered within milliseconds after a single 0.3-ms pulse. High-temperature samples had a more prolonged recovery time. Using time-resolved freeze fracture electron microscopy, aggregates of lipid vesicles were observed in all samples pulsed above the threshold voltage. The sizes and fractional areas occupied by aggregates of lipid vesicles at 4°C and at 25°C were measured at different time points after the applied pulse. Aggregates of vesicles persisted long after the electric resistance was recovered. After pulsing at the same voltage of 80 V, samples at 4°C were found to have slightly more extensive aggregate formation initially, but recovered more rapidly than those at 25°C. The more rapid recovery of the 4°C samples was likely due to a lower supra-threshold voltage. Viscoelastic instability propagation created by the pulse may also play a role in the recovery of the aggregates.

INTRODUCTION

Recent studies have pointed out the potential of electroporation for enhancing transdermal drug delivery (Prausnitz et al., 1993, Vanbever and Preat, 1995; Johnson et al., 1998). The outermost layer of the skin, the stratum corneum, represents the main barrier to molecular transport (Hadgraft and Guy, 1989; Bronaugh and Maibach, 1989), and is usually described as several densely packed layers of flattened, dead, keratinized cells embedded in a matrix of lipid bilayers, which consist of ceramides, cholesterol, and free fatty acids (Madison et al., 1987; Hadgraft and Guy, 1989; Schurer and Elias, 1992). The stratum corneum can be disrupted by electroporation: the application of short, high-voltage electric pulses. The voltage is localized across the stratum corneum; its resistance is much larger than that of the epidermal, dermal, and fatty tissue layers combined. The skin resistance rapidly decreases with voltage, eventually reaching a residue value when the applied voltage exceeds 20–80 V (Gallo et al., 1997). This pulse-induced permeability is suggested to be due to the capacitive breakdown of the intercellular lipid bilayers and corneocyte membranes, creating a conductive path straight through the stratum corneum (Chizmadzhev et al., 1995). Several attempts at the visualization of this process have been made. Localized regions of dye transport, 40–80 μm in diameter, have been observed after high-voltage pulse application in heat-stripped skin using fluorescence microscopy (Pliquett et al., 1996). Lipid vesicles and their aggregations, 5–30 μm in diameter, have been found in the lipidic regions of the stratum corneum after the pulse using freeze-fracture electron microscopy (Gallo et al., 1999). The exact mechanism of these structural changes and how they relate to pulse-induced skin permeability is still elusive.

It has been shown that heat treatment alone could also induce lipid vesicle formation and aggregation in stratum corneum, disruptions very similar to those found after exposure to electric pulse (Gallo et al., 1999). It had been suggested that vesicle aggregates induced by the pulse were related to the pulse-induced permeability changes found in the skin. Heat has also been observed to induce skin permeability changes (Golden et al., 1986; Ogiso et al., 1998). Heat gun treatment at 80–90°C can cause up to an 80% drop in post-treatment resistance that can last for hours (data not shown). If heat can also permeabilize the skin, forming similar disruptions as that of pulsed samples, the heat- and pulse-treated samples may share a similar mechanism of action. It may be that joule heating is responsible for the disruption of the skin after the initial pores are formed, presumably after the first several microseconds of the pulse (Pliquett et al., 1996). By our calculations (Gallo et al., 1999), joule heating by the pulse is not likely to have much effect unless it is localized.

Received for publication 20 July 2000 and in final form 10 October 2001.

Address reprint requests to Dr. Sek Wen Hui, Department of Molecular and Cellular Biophysics, Roswell Park Cancer Institute, Buffalo, NY 14263. Tel.: 716-845-8595; Fax: 716-845-8899; E-mail: sekwen.hui@roswellpark.org.

Stephen A. Gallo's present address is LECB, Division of Basic Sciences, NCI-FCRDC, National Institutes of Health, Frederick, MD 21702.

0006-3495/02/01/109/11 $2.00

It is expected that skin lipids in the fluid state will be more amenable to vesicle formation than lipids in a gel state because the van der Waals forces between the acyl chains is weaker in fluid bilayers, increasing its pliability (Nagle and Tristram-Nagle, 2000). Porcine stratum corneum has lipid, lipid-protein phase transitions at 60 and 70°C. It might be possible that the joule heating to above transition temperatures may help to create vesicles and thus produce disruptions that last much longer than the original electropores do. For temperatures to rise above these transitions during the pulse the current has to be very localized. It may be that initial electropore formation localizes the current and allows for heating during the duration of the pulse.

The localized joule heating as a cause of stratum corneum lipid disruption has not been proven directly, because such resolute measurements of local temperature are very difficult with our skin model systems. Instead, we examined the effect of skin temperature on the permeabilization of the stratum corneum during and after the pulse, using both electrical measurements and time-resolved electron microscopy. This is based on the hypothesis that increased temperatures will induce an increase in lipid fluidity, affecting the skin's response to the pulse. Conversely, lowered temperatures may decrease the amount of lipid in the fluid state, possibly preventing vesicle formation altogether. Examining the temperature effect on pulse-induced conductance and ultrastructural changes will indicate the contribution of heating to the electroporation of the skin.

MATERIALS AND METHODS

Stratum corneum preparation

The porcine skin was obtained from a local abattoir or from experimental animals of Dr. John Canty, Department of Medicine of the University at Buffalo. Both fresh and frozen-stored (−80°C) skin were used. Skin resistances have been measured before freezing and after thawing. The resistance seems to experience little loss from the freezing-thawing process (Kasting and Bowman, 1990). The stratum corneum (SC) was separated from the dermis and fat layer by heat stripping (Bouwstra et al., 1991). Briefly, a small piece of skin (~5 × 10 cm) was laid flat, wrapped in aluminum foil, and submersed in 65°C deionized water for 10 min. The stratum corneum was then carefully peeled from the underlying layer and stored in a cold room (4°C) in a desiccant jar for at least 24 h. There was no discernable difference between the electric properties of fresh and stored samples.

Impedance measurements

The electric impedance of the stratum corneum was measured using a vertical diffusion holder (Crown Glass Company, Somerville, NJ). Hydrated stratum corneum was placed between the two chambers, which were equipped with platinum wire electrodes and filled with Tris buffer (100 mM NaCl, 10 mM Tris, 1 mM EDTA, pH 7.4). The temperature of the chamber was controlled by its outer fluid jacket, which was connected to the circulating system of the support (Crown Glass Company). The larger, lower chamber also held a magnetic stirrer and a thermocouple. The temperature of the chamber containing the stratum corneum was maintained at any given point between 4° and 82°C.

The electric impedance of the stratum corneum before, during, and after the applied pulse was measured in a temporally resolved manner with the set-up depicted in Fig. 1. The pulse generator (HV) and the alternating current source (LV functional generator) were connected together to a voltage divider, containing a 2.2 kOhm load resistor (R_L) and the stratum corneum in series. The two voltage sources were isolated from each other by a 2.2 kOhm resistor (R_L*) and a voltage-limiting diode (Fig. 1). The low voltage source was used to measure pre-pulse and post-pulse resistance. The pulse signal (high voltage) was used to permeabilize (for ion conductance) the stratum corneum and to measure its resistance during the pulse. Two oscilloscopes were needed to measure the impedance during and after the pulse because of the difference in voltage resolutions of pulse and a.c. measurements. Both oscilloscopes were attached to V_o and V_s. A single, rectangular pulse of 10–150 V and 300 μs duration was applied to the chamber electrodes on the opposite side of the stratum corneum, superimposed on a low-voltage (600 mV, 0.3 kHz) square wave. The high-voltage signal triggered one oscilloscope to record the a.c. component across the skin and the load resistance, while the other recorded the pulse itself. The capacitance of the stratum corneum was assessed by the rising-decaying time of V_s in response to a square pulse V_o. The capacitive part of the stratum corneum impedance was determined to be insignificant in comparison to its resistive part. The resistance of the stratum corneum, R_s, was then computed as

$$R_s = R_L V_s/(V_o - V_s) \quad (1)$$

The error in these resistance measurements was assessed using a standard 22 kOhm resistor in place of the stratum corneum. The calculated resistance yielded an average of 20 ± 4 kOhm from repeated pulsing at different voltages, giving an error of 20%. The residual resistance of the chamber, consisting of the resistance of the electrodes and buffer solution, was measured with the SC deliberately perforated by needles after experiment. The residual resistance was typically 1–2 kOhm, contributing to ~10% of the SC resistance before electroporation. The rapid fluctuation in R_s in Fig. 4 was caused by the digital oscilloscope recordings of V_o and V_s, especially when the values of V_o and V_s were similar.

Freeze-fracture electron microscopy

Time-resolved freeze-fracture electron microscopy (TFEM) was used to visualize porcine stratum corneum frozen immediately after the application of an electric pulse. The technique is described in detail elsewhere (Gallo et al., 1999). Briefly, pieces of stratum corneum 1.5 mm in diameter were hydrated with filtered water for 5 min and then were sandwiched between two thin copper plate electrodes, which also acted as cooling contacts. The electrode separation was controlled using 25-μm-thick Mylar spacers. The experiment was conducted either at room temperature (25°C) or in a cold room (4°C). The sample was allowed a minute to equilibrate to the appropriate temperature. The sample was pulsed at set times of 0.5 ms, 12 ms, 5 s, and 5 min before freezing, at a voltage of 80 V and a pulse length of 300 μs. These time points represent the beginning of cryofixation, which takes <2 ms to complete for samples of this thickness. For each time point a data set of three to eight repeat samples was collected. Freeze-fracture electron microscopy was then conducted to observe the ultrastructural changes in the skin and quantify their size and the frequency of their appearance.

RESULTS

Impedance measurements

The instantaneous change of resistance during pulse was calculated from the simultaneous measurements of V_o and V_s tracings using Eq. 1, and plotted in Fig. 2. At low pulse

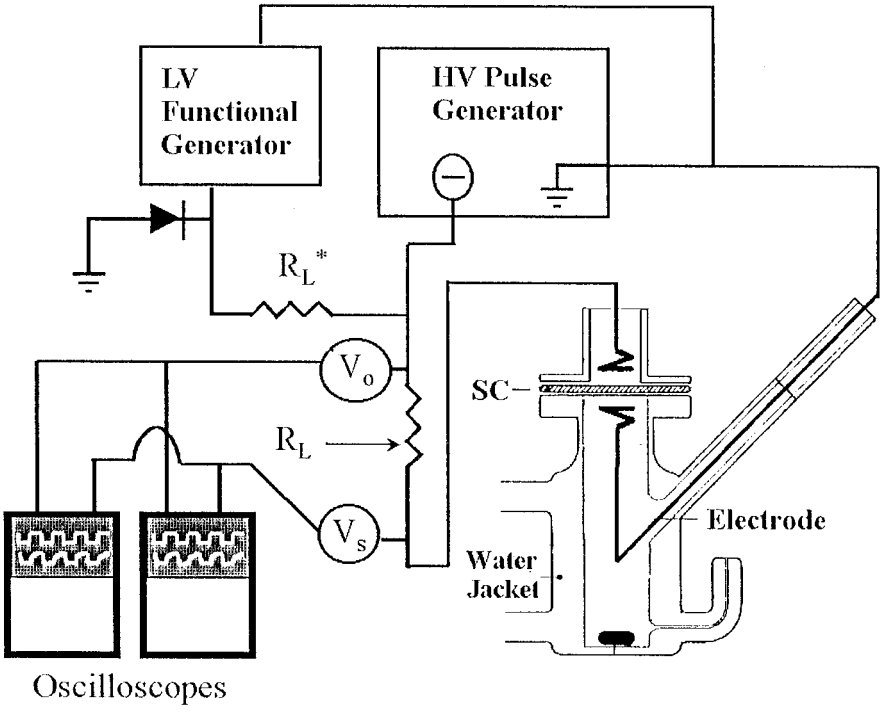

FIGURE 1 Electrical set-up for measuring the resistance of porcine stratum corneum, which was placed between two chambers of the vertical diffusion holder. The high-voltage pulse generator was used to apply the pulse treatment and to measure the resistance during the pulse using a voltage divider and an oscilloscope. The low-voltage function generator was used for pre/post-pulse resistance measurement. The low- and high-voltage generators were isolated from each other by a voltage-limiting diode and a resistor R_L*. The signals were superimposed to measure resistance continuously during and immediately after the pulse. Two oscilloscopes were used, one to detect the high-voltage pulse and the other one to measure resistance by low-voltage a.c. square wave.

voltages the apparent resistance dropped precipitously at the beginning of the pulse, due to the charging of the stratum corneum capacitor, indicating that the stratum corneum remains largely unpermeabilized. The apparent resistance returned to a value slightly less than the initial resistance throughout the rest of the pulse. At a higher pulse voltage the residue resistance assumed a constant and lower value for the rest of the pulse, indicating a partial breakdown of the stratum corneum. The measured voltage across the SC, V_s, which led to such response, is referred as the threshold voltage. At higher voltages the apparent resistance stayed at a value that was close to the residue resistance of the chamber, signifying a complete breakdown of the stratum corneum throughout the pulse. The relative resistance drop (R_s/R_o) would appear to be more pronounced if the residue resistance of the chamber was subtracted from the measured values of R_s. At each temperature the higher the applied pulse voltage, the greater the percentage resistance drop, until reaching a transition voltage above which the percentage resistance drop became less dependent on voltage (Fig. 3 *A*). The best-fit trend lines for these two phases of resistance change intercepted at a transition voltage value that was usually the same as the threshold value. With the drop of SC resistance during the pulse, the voltages V_o and V_s redistributed. The voltage $V_s(0)$ initially experienced by the SC at the beginning of the pulse could be calculated by Eq. 1, using the pre-pulse value of R_s. When the threshold voltage and the corresponding initial voltage $V_s(0)$ were plotted against the temperature of the stratum corneum, as

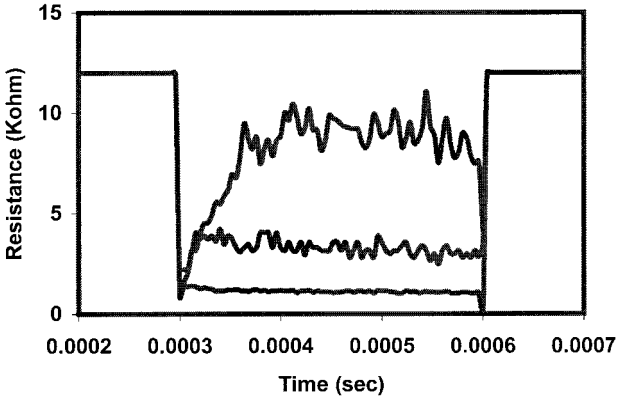

FIGURE 2 Instantaneous apparent resistance change during a 0.3-ms pulse, at measured V_s of 34 V (*top*), 54 V (*middle*), and 88 V (*bottom*), corresponding to initial voltages $V_s(0)$ of 43 V, 104 V, and 284 V, respectively. The apparent resistances were calculated from oscilloscope tracings of V_o and V_s. The sample was kept at 40°C, corresponding to a threshold voltage of 57 V and an initial permeabilizing voltage of 113 V.

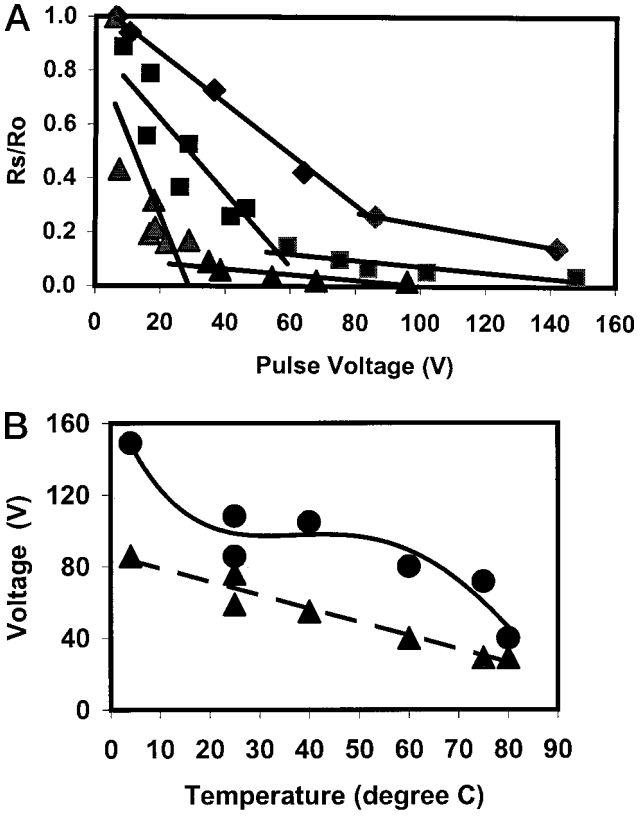

FIGURE 3 (*A*) Relative stratum corneum resistance (R_s/R_o) reduction during pulse versus pulse voltage at different sample temperatures. Resistances were measured during the 0.3-ms pulse at 4°C (♦), 25°C (■), and 80°C (▲). Trend lines represent linear best fit. (*B*) The threshold voltage, V_s (▲), observed from resistance drop (as shown in Fig. 2), and from the transition points of two phases of resistance change (as shown in Fig. 3 *A*), as well as the corresponding initial permeabilizing pulse voltages $V_s(0)$ (●) are plotted against temperature. Lines are from best fit calculation.

shown in Fig. 3 *B*, they showed a general decreasing trend with increasing temperature. The initial voltage that led to the breakdown of the SC showed a large drop at temperatures >70°, the putative transition temperature of the SC sphingolipid.

The recovery of the stratum corneum from the pulse was also affected by temperature. The normalized post-pulse resistance after exposure to an 80–96 V, 300 μs pulse was computed and plotted against time at 4°, 25°, and 82°C (Fig. 4). The resistance regained most of its initial value in milliseconds after a large drop during the pulse. An initial phase of recovery usually occurred within 10 ms, and subsequently the resistance showed a small and irregular oscillation that was eventually damped out at ~50 ms. Samples pulsed at lower temperature and low pulse voltage tended to have shorter total recovery time, but the relation was not well-defined due to the small variation of resistance at the end of the recovery period. To compare the recovery times from samples pulsed at different voltages and temperatures, the initial and total recovery times of pulsed samples were plotted in terms of their supra-threshold voltage (pulse voltage in excess of the threshold voltage at each sample temperature, as defined in Fig. 3 *B*). The result is given in Fig. 5. It shows that the total recovery time increased, in general, with increasing supra-threshold voltages. The initial phase of recovery was independent of temperature and pulse voltage, as long as it was higher than the threshold voltage. Otherwise, it was zero, i.e., there was no change in resistance from that before pulse.

Freeze-fracture electron microscopy

Freeze fracture studies indicate that stratum corneum temperature influences vesicle formation and their kinetics in pulsed samples. At both cold room (4°C) and room temperature (25°C), multi or unilamellar vesicles of various sizes (0.1–3 μm) were found to aggregate in the lamellar lipid region or confined hydrated areas of the stratum corneum. These aggregates varied from 1 μm to 50 μm across (Figs. 6, *A–D* and 7, *A–D*). The morphological changes in the stratum corneum for each temperature condition were quantified by five parameters: aggregate density, fractional aggregate area, individual aggregate area, number of vesicles per aggregate, and vesicle diameter. The aggregate density (Fig. 8) and the fractional aggregate area (Fig. 15) were quantified by the total number of aggregates or the combined area of all the aggregates, respectively, divided by the total replica area surveyed for each time point, typically ranging from 2 to 8×10^6 μm^2. Histograms were obtained in terms of the last three parameters and were displayed in three-dimensional plots to illustrate the time evolution (Figs. 9–14). The histograms were normalized by the total replica area surveyed for each sample, typically ranging from 0.1 to 3.4×10^6 μm^2.

In the room temperature experiments, aggregations of vesicles were found at 0.5 ms post-pulse. Aggregate density rose until it reached an apex of 4.5×10^{-6} μm^{-2} at 5 s, and persisted to 5 min (Fig. 8). The aggregate size distribution at 0.5 ms was skewed toward small areas, 25–50 μm^2. These smaller aggregates increased in number and the distribution became more skewed with time until the apex at 5 s, past which the distribution spreads out to reach 600 μm^2 (Fig. 9). The fractional aggregate area dropped from 0.1% to 0.01% in the first several milliseconds, then slowly rising back to 0.1% by 5 min (Fig. 15).

The distribution of the number of vesicles per aggregate became skewed to lower numbers by 12 ms due to an increase in aggregates containing 10–20 vesicles. The trend continued at the 5 s time point, but by 5 min the distribution had spread out to reach 80 vesicles per aggregate (Fig. 10). The vesicle size distribution was centered around 1.5 μm in diameter at 0.5 ms. At 12 ms the distribution became slightly skewed toward 1.0 μm. At longer time points, the distribution resembled that of 0.5 ms (Fig. 11).

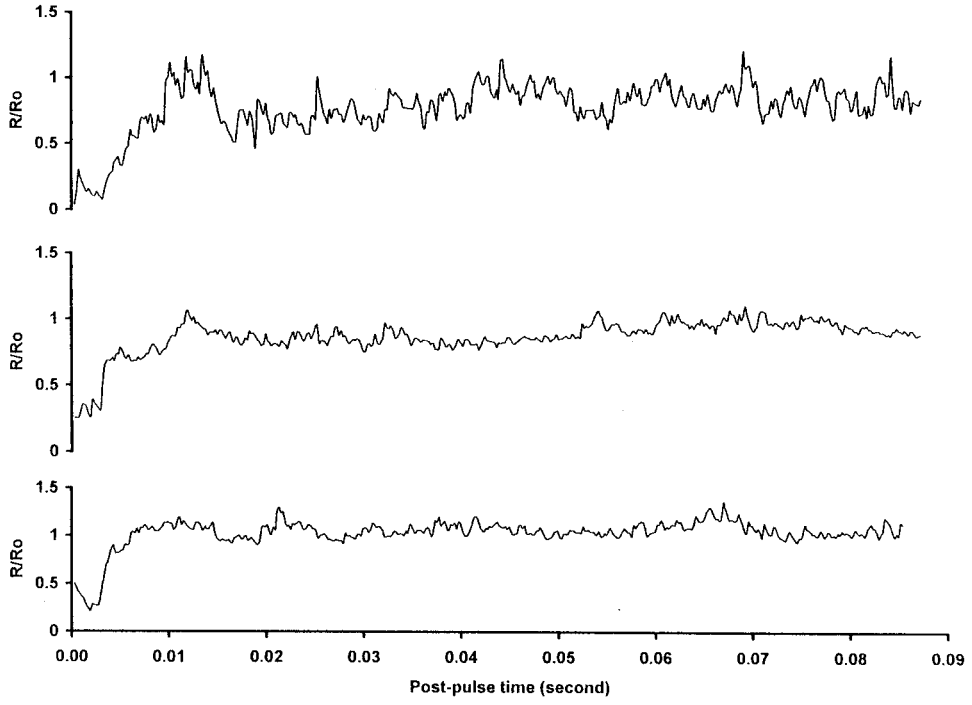

FIGURE 4 Continuous registration of the stratum corneum resistance after pulsing. Post-pulse resistance was computed immediately after the pulse using continuous recordings for V_o and V_s at different sample temperatures. Samples were pulsed once with a 0.3-ms pulse with V_s equal to 86 V at 4°C (*bottom*), 80 V at 25°C (*middle*), and 96 V at 82°C (*top*).

In the cold room experiments the aggregate density is at its highest, 5×10^{-6} μm^{-2}, at 0.5 ms. This density steadily decreases until 5 s, where it stays at $\sim 0.5–1.5 \times 10^{-6}$ μm^{-2} for the next 5 min (Fig. 8). The aggregate size distribution is quite flat at 0.5 ms and 12 ms, reaching aggregate areas of 1500 μm^2 (Fig. 12). The number of aggregates then decreases, the aggregate area becoming skewed toward 25–50 μm^2. The fractional area is at a maximum of ~0.25% through 12 ms, at which point it rapidly decreases to ~0.01%, remaining there for minutes (Fig. 15). The number of vesicles per aggregate ranged from 10 to 90 vesicles, and the distribution was quite flat until the 5 s time point, at which it became skewed toward 15–20 vesicles and remained that way up to 5 min after the pulse (Fig. 13). The vesicle size distribution was centered ~1.0 μm throughout all time points (Fig. 14).

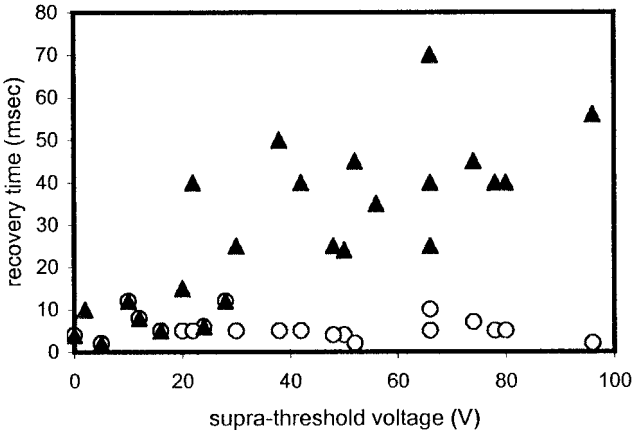

FIGURE 5 The initial phase (○) and total recovery times (▲) of stratum corneum resistance plotted as functions of supra-threshold voltage after experiencing a single 0.3 ms pulse.

DISCUSSION

Although many investigators have observed the enhancement of molecular flux (Prausnitz et al., 1993; Vanbever and Preat, 1995; Johnson et al., 1998), the mechanism of pulse-induced permeabilization of the stratum corneum is still not proven experimentally. Electroporation of the stratum corneum lipid bilayers is likely to occur, provided the applied field is sufficient (Pliquett et al., 1995), but the electric breakdown of lipid bilayers may not be the only factor at work. The pulse provides external energy, which is partly dissipated through the joule heating of the stratum corneum. It has been found that heat treatment alone induces reductions in skin resistance (data not shown). The effect of bulk heat treatment on molecular flux, mechanical properties, resistance, and lipid ultrastructure has been studied extensively (Wilkes and Wildnauer, 1973; Golden et al., 1986; Oh et al., 1993; Panescu et al, 1994; Ogiso et al.,

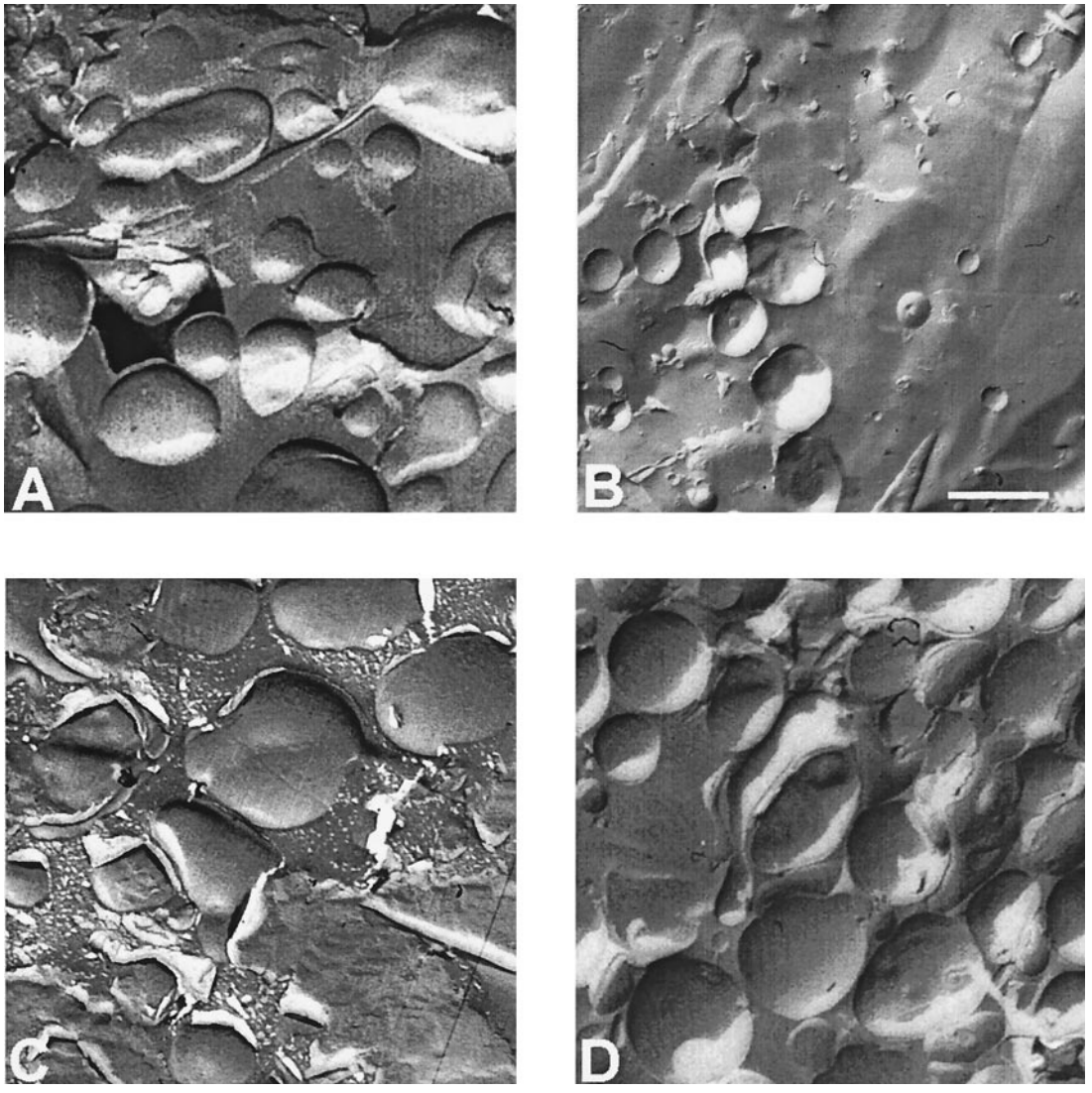

FIGURE 6 Freeze-fracture electron micrographs of 25°C porcine stratum corneum samples pulsed for 300 μs with V_s = 80 V. Samples were pulsed at (*A*) 0.5 ms, (*B*) 12 ms, (*C*) 5 s, and (*D*) 5 min before freezing. The bar equals 1 μm.

1998; Gallo et al., 1999). Recently, localized temperature gradients (105 K/m) have been found in skin after high-voltage pulse application (Pliquett and Gusbeth, 2000). These areas seem to coincide with the localized transport regions found also in the skin after pulsing (Pliquett et al., 1996). Ultrastructural studies carried out previously have revealed aggregates of multilamellar vesicles, after exposure of the skin to the pulse, which seem to correspond to the localized transport regions (Gallo et al., 1999). Heat treatment was also found to initiate aggregate formation. It may be that lipid fluidity plays a role in the disruption of the stratum corneum, a factor controlled by temperature. General lipid disorder has been found in the stratum corneum after exposure to multiple pulses, and disordering of the lipid lamellae has been detected in samples undergoing prolonged iontophoresis (Jadoul et al., 1996, 1998). The work presented here, along with previous studies, was analyzed in an attempt to address the importance of temperature in electroporation-induced perturbations in the stratum corneum.

Electrical measurements were conducted on heated and cooled samples to observe how temperature would affect the resistance changes during the pulse and recovery after the pulse. When compared with electrical measurements of human SC and skin at room temperature by Pliquett et al. (1995), our results differ somewhat with theirs in terms of relative percentage resistance drop and recovery time. The difference is likely due to the longer pulses and thicker specimens of human skins they used. We found that temperature did have a significant effect on the resistance drop during the pulse. Permeabilizing voltages that the SC experienced decrease with increasing temperature (Fig. 3 *B*).

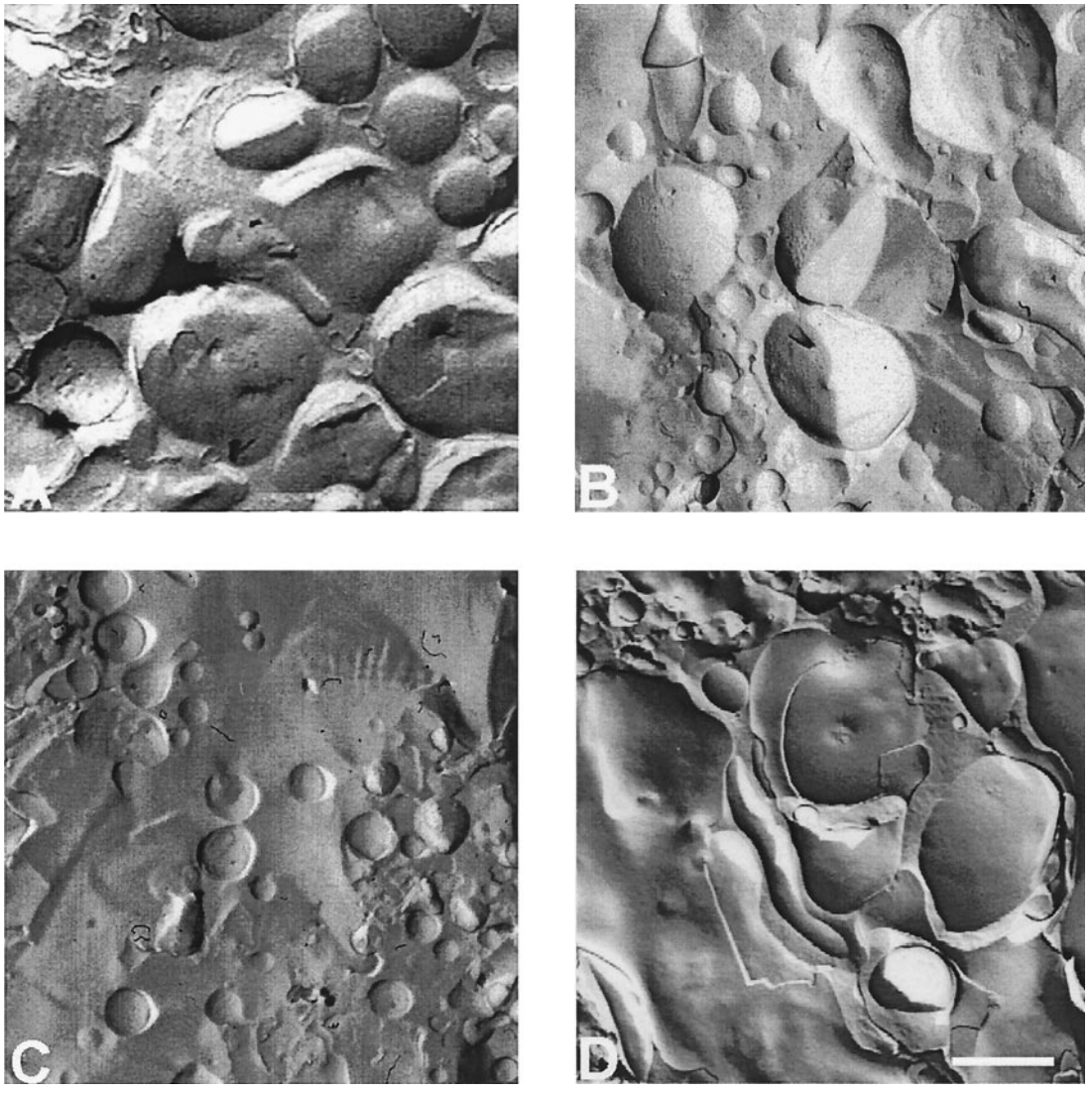

FIGURE 7 Freeze-fracture electron micrographs of 4°C porcine stratum corneum samples pulsed for 300 μs with V_s = 80 V. Samples were pulsed at (*A*) 0.5 ms, (*B*) 12 ms, (*C*) 5 s, and (*D*) 5 min. The bar equals 1 μm.

Furthermore, the higher the temperature, the steeper the relative resistance drop with increasing voltage (Fig. 3 *A*). The voltages that mark the transition between two phases of resistance drop coincide with the threshold voltages required to permeabilize the SC during the pulse. At pulse voltages higher than the threshold, $\Delta R/\Delta V$ becomes lower, indicating an increase in trans-SC current (Δi) due to the permeabilization of the SC. The fact that increasing temperature rendered the permeabilizing voltage lower indicates that elevated temperatures facilitated the formation of electropores. If the stratum corneum has a spontaneous pore-forming temperature, then high temperature samples require less electric energy to reach this temperature locally.

This change may also affect the resealing of the pores. The initial recovery phase, which typically lasted ~5 ms (Figs. 4 and 5), was most likely due to the reseal of the

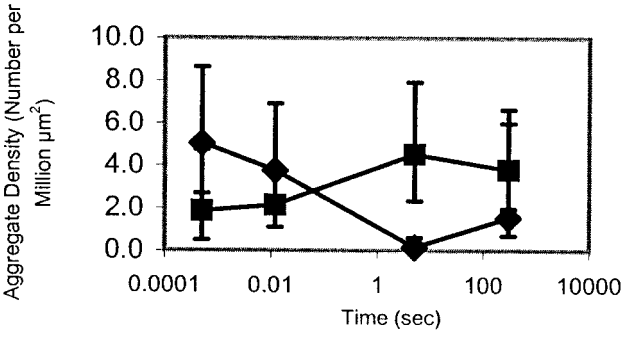

FIGURE 8 Plot of aggregate density for 4°C (*diamonds*) and 25°C (*squares*). The total number of aggregates divided by the total observed replica area is plotted against time (in logarithmic scale) after pulse application. The number of samples per time point ranged from three to eight.

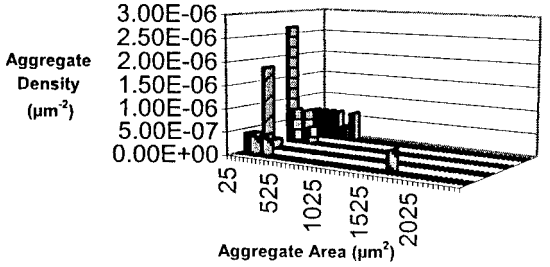

FIGURE 9 Three-dimensional histogram analysis of the aggregate density (for the 25°C samples) according to the aggregate size and its time evolution. Data for 0.5 ms, 12 ms, 5 s, and 5 min time points are plotted from front to back, respectively (same order as in Figs. 10–14). The number of aggregates divided by the total observed area per time point is plotted against aggregate area.

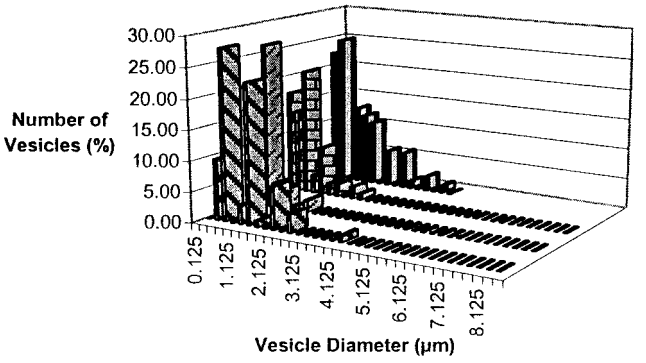

FIGURE 11 Three-dimensional histogram analysis of the number of vesicles (for the 25°C samples) according to the vesicle diameter and its time evolution. The percentage of the total number of vesicles per time point is plotted against vesicle diameter.

primary electropores. These primary electropores, expected to be only nanometers in diameter, were probably not observable even by time-resolved freeze-fracture electron microscopy. Subsequent recovery of the resistance lasting up to 50 ms was likely to relate to the gradual resealing of the secondary conductive path contributed by aggregates of lipid vesicles in the stratum corneum. Depending on their interconnectivity, these aggregates may affect the patterns of post-pulse resistance recovery, including the weak oscillations in resistance. The second phase of recovery tended to be longer when the voltages of the applied pulses were higher than the respective threshold voltage for that temperature (Fig. 5). It is possible that the supra-threshold voltage contributed to more extensive or more numerous damage areas, leading to longer recovery time of residual (secondary) damages. Because the threshold voltage is approximately inversely proportional to the threshold temperature, it translates to the relation that the secondary recovery time increases also with supra-threshold temperature. In other words, for the same pulse voltage, 4°C samples experienced lower supra-threshold voltage than did 25°C samples, hence the recovery is more rapid. Freeze-fracture experiments were then conducted to determine whether this relationship translated into vesicle aggregate formation.

The freeze-fracture experiment at room temperature yielded vesicle aggregates already at 0.5 ms after the pulse (Fig. 6 *A*). In the cold room experiment a large number of aggregates, 5×10^{-6} μm^{-2}, form by the first 0.5 ms (Figs. 7 *A* and 8). These large aggregates (Fig. 12) contain a large number of vesicles (Fig. 13), and maintain a fractional area of ~0.25% for the first several milliseconds after the pulse (Fig. 15). The room temperature samples have a slightly, though not significantly, lower fractional area of aggregates of 0.12%, and contain smaller aggregates (Fig. 9) and fewer numbers of vesicles per aggregate (Fig. 10). This slight difference may be due to the initial compression of the micro-areas at potential breakdown sites of the membrane by the electric field. The local compression created by the

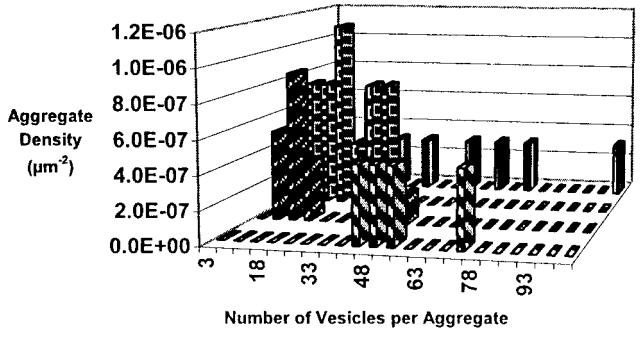

FIGURE 10 Three-dimensional histogram analysis of the aggregate density (for the 25°C samples) according to the number of vesicles per aggregate and its time evolution. The number of aggregates divided by the total observed area per time point is plotted against vesicle number.

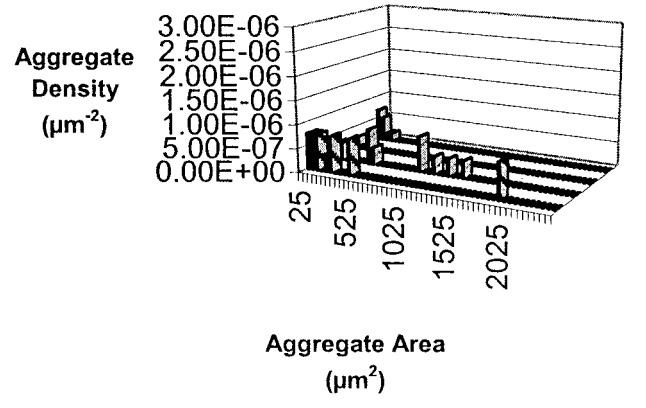

FIGURE 12 Three-dimensional histogram analysis of the aggregate density (for the 4°C samples) according to the aggregate size and its time evolution. The number of aggregates divided by the total observed area per time point is plotted against aggregate area.

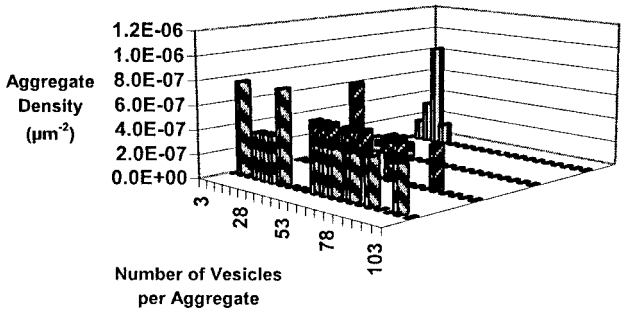

FIGURE 13 Three-dimensional histogram analysis of the aggregate density (for the 4°C samples) according to the number of vesicles per aggregate and its time evolution. The number of aggregates divided by the total observed area per time point is plotted against vesicle number.

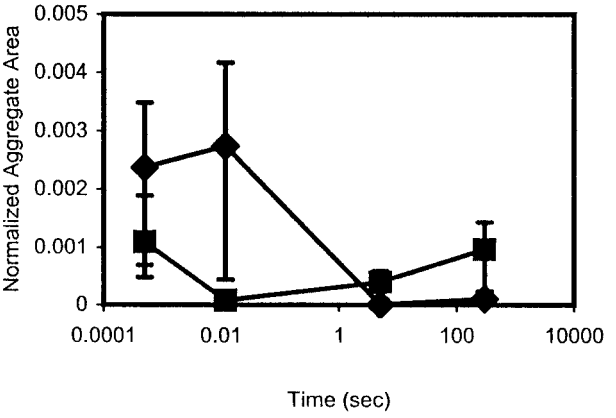

FIGURE 15 Plot of normalized aggregate area for 4°C (*diamonds*) and 25°C (*squares*). The combined area of all aggregates divided by the total observed replica area is plotted against time (in logarithmic scale) after pulse application. The number of samples per time point ranged from three to eight.

electric field can be related to the expansivity modulus, K, by the following expression:

$$(1/2)\epsilon_m\epsilon_o(V^2/h_o) = K\alpha \quad (2)$$

where V is the applied voltage, h_o is the initial thickness of the stratum corneum bilayers, α is the relative increase in local micro-area of the membrane, and ϵ_m and ϵ_o are the dielectric constants of the membrane and free-space, respectively (Needham and Hochmuth, 1989). For a given voltage, a larger modulus will translate to a smaller increase in micro-area. It has been shown that human stratum corneum undergoes a mechanical transition at 0–10°C (Wilkes and Wildnauer, 1973), suggested to be associated with the mobility of water. The Young's modulus increases up to an order of magnitude with the decrease in temperature from 25°C to 4°C. Therefore, the relative increase in local micro-area (α) must be restricted proportionally, so that the local energy density is higher in the 4°C samples, which lead to the creation of larger aggregate areas and densities. Mechanical energy can create vesicles from multilamellar states, as seen in the sonication and vortexing processes in liposome preparation. This is also an energy-dependent process.

A different process governs the recovery of vesicle aggregates to the lamellar state. The aggregate density in the 4°C samples continually decreases after the 12 ms time point, until it levels out at 0.5–1.5 $\times$ 10^{-6} μm^{-2}, seconds to minutes after the pulse (Fig. 8). The fractional area greatly decreases after the 12 ms time point, from 0.25% to $<$0.01%, resulting from diminishing aggregate areas (Fig. 12) and vesicle numbers (Fig. 13), vesicle size remaining constant (Fig. 14). This is different from the room temperature data, where the aggregate density gradually rises to its apex 5 s after the pulse, aggregate areas becoming smaller during this period (Fig. 8). These small aggregates (Figs. 9–11) remain at about this level for minutes (Fig. 15). A possible explanation of the difference between the two temperatures is given below. The energy equation governing the vesicle formation from lamellae is presented in Eq. 3. It may be assumed that the elastic energy density (g_{el}) of a multilamellar system is given by:

$$g_{el} = (k/2)(1/R - 1/R_o)^2 \quad (3)$$

where k is the rigidity constant of the membrane, R_o is the spontaneous curvature, and R is the actual curvature of the membrane (Helfrich, 1973). This represents the stress the membrane feels when bent beyond its natural state. The rigidity constant is dependent on the state and composition of the lipid. Because these vesicles have been observed to eventually revert back to the lamellae state (Gallo et al., 1999), it is assumed that the value of R_o is close to infinity. The rigidity constant (k) is assumed to be higher at lower temperatures, increasing the energy expenses necessary to bend the membrane. The vesicles become less stable and fuse back into the lamellae state more readily. Room temperature samples do not recover from the pulse as quickly

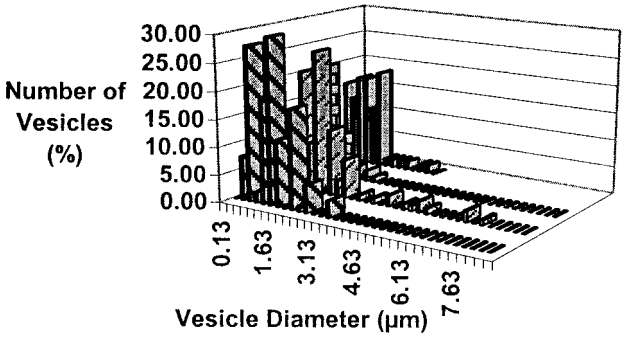

FIGURE 14 Three-dimensional histogram analysis of the number of vesicles (for the 4°C samples) according to the vesicle diameter and its time evolution. The percentage of the total number of vesicles per time point is plotted against vesicle diameter.

because the applied pulse voltage (80 V) is farther above the corresponding threshold voltage (68 V), and therefore take longer to recover.

The freeze-fracture data and the resistance recovery data bear a similarity to each other in the sense that the 4°C samples recover faster than the 25°C samples, but the resistance recovery is in milliseconds while the aggregates take at least minutes to revert to lamellae. We do not know the exact relation between electric conductivity and vesicle aggregate formation. Furthermore, with the present set-up, no information can be extracted from these experiments about the depth of these aggregates into the stratum corneum, nor is there any information concerning the connectivity of these aggregates in the third dimension. It may be that the connections between permeabilized areas seal before the vesicle aggregates do. Once one layer is sealed, the resistance will increase significantly, even if many vesicles still exist in other layers.

The aggregate size in the 25°C samples drops in the first few milliseconds. At the same time, both vesicle size and number decreasing (Figs. 9–11 and 15). The fractional aggregate area then increases in seconds with the increase in vesicle size and number. This initial drop and rebound may be related to mechanical compression waves squeezing the viscoelastic stratum corneum, possibly created by electrocompression and subsequent heating. The disruption is not unlike the permeabilization of the skin by ultrasonic waves (Mitragotri et al., 1995). The relaxation time of viscoelastic liquid membranes by small wave instabilities, using a Maxwell model, has been calculated to be directly proportional to the viscosity, and is estimated to be on the order of seconds for highly viscous membranes (Steinchen et al., 1981). The relaxation time of the skin from electric stresses has been predicted for fast and slow areas of recovery as milliseconds and several seconds, respectively (Pawlowski et al., 1998). These values represent a similar time scale to that of the shrinking and enlarging of the aggregates. The more rigid 4°C samples may revert to the lamellar state faster than this time scale, causing large amounts of vesicle fusion, damping the viscoelastic waves in these samples, and shorten the total recovery time (Fig. 5).

Despite the differences in these two sets of data, 4°C and 25°C, a common feature is that aggregates of vesicles do form in all samples. Temperature measurements suggest localized regions of human stratum corneum experience large thermal gradients during the pulse, reaching temperatures above the phase transition temperatures of the sphingolipids (Pliquett and Gusbeth, 2000). It may be necessary for the lipids to undergo these transitions for vesicle aggregations to form. If this is true, the local temperatures created by the pulse seem to be more than sufficient to cause the lipid melting even at 4°C.

Because of the slow rise in aggregate density, the perturbations seen in the freeze-fracture studies are likely to be a secondary reaction to the pulse (Gallo et al., 1999). The initial disturbance could be much smaller. If this small cross-sectional area represents the pathway by which the initial current flows, the current density could be quite high during the pulse, allowing for a significant amount of heating to take place. If this heating is responsible for aggregate formation, it may be responsible for the severe disruption of the stratum corneum by the pulse. These data suggest that a heating model is incomplete without consideration of the viscoelasticity of the stratum corneum. Thus, the more that is understood about the mechanism of high-voltage pulsing on stratum corneum, the better we can optimize the treatment parameters for transdermal drug delivery.

The authors thank Dr. John Canty, of the Department of Medicine at SUNY at Buffalo, who supplied some of the porcine skin for this project. The time-resolved freezing device was fabricated by Brian Chow and George Potienko. The vertical diffusion chambers and perfusion platform were on loan from the Department of Pharmaceutics, SUNY at Buffalo. Statistical analysis was performed with the help of Dr. William Greco, Biostatistics Facility, which is supported by CCSG Grant CA 16056 from the National Cancer Institute.

This work is supported by Grant GM 55864 from the National Institutes of Health.

REFERENCES

Bouwstra, J. A., G. S. Gooris, J. A. Van der Spek, and W. Bras. 1991. Structural investigations of human stratum corneum by small-angle x-ray scattering. *J. Invest. Dermatol.* 97:1005–1012.

Bronaugh, R. L., and H. I. Maibach. 1989. Percutaneous Absorption: Mechanisms—Methodology—Drug Delivery. Marcel Dekker, New York.

Chizmadzhev, Y., V. Zarnytsin, J. C. Weaver, and R. O. Potts. 1995. Mechanism of electroinduced ionic species transport through a multi lamellar lipid system. *Biophys. J.* 68:749–765.

Gallo, S. A., A. R. Oseroff, P. G. Johnson, and S. W. Hui. 1997. Characterization of electric-pulse-induced permeabilization of porcine skin using surface electrodes. *Biophys. J.* 72:2805–2811.

Gallo, S. A., A. Sen, M. L. Hensen, and S. W. Hui. 1999. Morphological changes to porcine stratum corneum following an electric pulse. *Biophys. J.* 76:2824–2832.

Golden, G. M., D. B. Guzek, A. H. Kennedy, J. E. Mckie, and R. O. Potts. 1986. Stratum corneum lipid phase transitions and water barrier properties. *Biochemistry.* 26:2382–2388.

Hadgraft, J., and R. H. Guy. 1989. Transdermal Drug Delivery, Developmental Issues and Research Initiatives. Marcel Dekker, New York.

Helfrich, W. 1973. Elastic properties of lipid bilayers: theory and possible experiments. *Z. Naturforsch.* 28C:693–703.

Jadoul, A., J. Doucet, D. Durand, and V. Preat. 1996. Modifications induced on stratum corneum structure after in vitro iontophoresis: ATR-FTIR and x-ray scattering studies. *J. Controlled Release.* 42:165–173.

Jadoul, A., H. Tanojo, V. Preat, J. Bouwstra, F. Spies, and H. Bodde. 1998. Electroperturbation of human stratum corneum fine structure by high voltage pulses: a freeze-fracture electron microscopy and differential thermal analysis study. *J. Invest. Dermatol. Symp. Proc.* 3:153–158.

Johnson, P. G., S. A. Gallo, S. W. Hui, and A. R. Oseroff. 1998. A pulsed induced electric field enhances cutaneous delivery of methylene blue in excised full-thickness porcine skin. *J. Invest. Dermatol.* 11:457–463.

Kasting, G. B., and L. A. Bowman. 1990. Electrical analysis of fresh, excised human skin: a comparison with frozen skin. *Pharm. Res.* 7:1141–1146.

Madison, K. C., D. C. Swartzendruber, P. W. Wertz, and D. T. Downing. 1987. Presence of intact intercellular lipid lamella in the upper layers of the stratum corneum. *J. Invest. Dermatol.* 88:714–718.

Mitragotri, S., D. Edwards, D. Blankschtein, and R. Langer. 1995. A mechanistic study of ultrasonically-enhanced transdermal drug delivery. *J. Pharm. Sci.* 84:697–706.

Nagle, J. F., and S. Tristram-Nagle. 2000. Structure of lipid bilayers. *Biochim. Biophys. Acta.* 1469:159–195.

Needham, D., and R. M. Hochmuth. 1989. Electromechanical permeabilization of lipid vesicles. *Biophys. J.* 55:1001–1009.

Ogiso, T., T. Hirota, M. Iwaki, T. Hino, and T. Tanino. 1998. Effect of temperature on percutaneous absorption of terodiline, and relationship between penetration and fluidity of the stratum corneum lipids. *Int. J. Pharmacol.* 176:63–72.

Oh, S. Y., L. Leung, D. Bommannan, R. H. Guy, and R. O. Potts. 1993. Effect of current, ionic strength and temperature on the electrical properties of skin. *J. Controlled Release.* 27:115–125.

Panescu, D., J. G. Webster, and R. A. Stratbucker. 1994. A non-linear electrical-thermal model of the skin. *IEEE Trans. Biomed. Eng.* 41: 672–679.

Pawlowski, P., S. A. Gallo, P. G. Johnson, and S. W. Hui. 1998. Electrorheological modeling of the permeabilization of stratum corneum: theory and experiment. *Biophys. J.* 75:2721–2731.

Pliquett, U. F., and C. H. Gusbeth. 2000. Perturbation of human skin due to application of high voltage. *Bioelectrochemistry.* 51:41–51.

Pliquett, U. F., R. Langer, and J. C. Weaver. 1995. Changes in the passive electrical properties of human stratum corneum due to electroporation. *Biochim. Biophys. Acta.* 1239:111–121.

Pliquett, U. F., T. E. Zewert, T. Chen, R. Langer, and J. C. Weaver. 1996. Imaging of fluorescent molecule and small ion transport through human stratum corneum during high voltage pulsing: localized transport regions are involved. *Biophys. Chem.* 58:185–204.

Prausnitz, M., V. Bose, R. Langer, and J. C. Weaver. 1993. Electroporation of mammalian skin: a mechanism to enhance transdermal drug delivery. *Proc. Natl. Acad. Sci. U.S.A.* 90:10504–10508.

Schurer, N. J., and P. M. Elias. 1992. The biochemistry and function of stratum corneum lipids. *Adv. Lipid Res.* 24:27–56.

Steinchen, A., D. Gallez, and A. Sanfeld. 1981. A viscoelastic approach to the hydrodynamic stability of membranes. *J. Colloid Interface Sci.* 85:5–15.

Vanbever, R., and V. Preat. 1995. Factors affecting transdermal delivery of metoprolol by electroporation. *Bioelectrochem. Bioenerg.* 38:223–228.

Wilkes, G. L., and R. H. Wildnauer. 1973. Structure-property relationships of the stratum corneum of the neo-natal rat II. *Biochim. Biophys. Acta.* 302:276–289.